Supporting Information for "It's Not Easy Being Green: Kinetic Modeling of the Emission Spectrum Observed in STEVE's Picket Fence"

L. Claire Gasque[1], Reza Janalizadeh[2], Brian J. Harding[1], Justin D. Yonker[3],

D. Megan Gillies[4]

[1]University of California, Berkeley, Space Sciences Laboratory

[2]The Pennsylvania State University, Department of Electrical Engineering

[3]The Johns Hopkins University Applied Physics Laboratory

[4]University of Calgary, Physics and Astronomy Department

Contents of this file

Introduction

The supporting information below contains details of the kinetic modeling used to determine volume emission rates (VERs) for various spectral features under the influence of electric fields parallel to the magnetic field in a realistic atmosphere.

Text S1 describes the detailed modeling needed for the main results of the paper: determining whether, using a kinetic model driven only by parallel electric fields, it is possible to obtain the observed ratio of N_2 1st positive (N_2 1P) to Oxygen 557.7 nm green line (GL) emissions while simultaneously not producing N_2^+ first negative (N_2^+ 1N) emissions. Tables S1 and S2 give the rates used for the quenching reactions and radiative cascade, respectively. Figure S1 presents the atmospheric and ionospheric density profiles used in the modeling.

Text S2 describes an extension of this modeling to predict whether, under this mechanism, emission features in the ultra-violet (UV) spectral range might be observable in space-based observations of the picket fence. The detailed results of this analysis are shown in Figure S2.

Text S1. Detailed Steady State Kinetic Calculations of N_2 1P and GL VERs

Atmospheric and ionospheric density profiles used in the modeling described in this section are shown in Figure S1.

N_2 1P emissions are produced through the rapid relaxation of the $N_2\,(B^3\Pi_g)$ state to the $N_2\,(A^3\Sigma_u^+)$ state. Atmospheric quenching effects are negligible. Radiative cascade from higher energy states, including $N_2\,(W^3\Delta_u)$, $N_2\,(B'^3\Sigma_u^-)$, and $N_2\,(C^3\Pi_u)$, significantly contribute to the total $N_2\,(B^3\Pi_g)$ population (Vallance Jones, 1974). Only half of the population excited by electron impact in the $N_2\,(C^3\Pi_u)$ state contributes to the cascade due to a pre-dissociation branching ratio of 0.5 (Porter et al., 1976). Contributions from the

$N_2\left(E^3\Sigma_g^+\right)$ and $N_2\left(D^3\Sigma_u^+\right)$ states, which have small excitation cross sections, are omitted, following Meier (1991). Considering that we do not resolve individual vibrational levels of N_2, contributions from reverse first positive transitions, which comprise the relaxation of higher vibrational levels of $N_2\left(A^3\Sigma_u^+\right)$ to lower vibrational levels of $N_2\left(B^3\Pi_g\right)$, are also omitted. The N_2 1P VER is obtained by summing the direct electron impact excitation rate and the rate of radiative cascade to the $N_2\left(B^3\Pi_g\right)$ state. Balancing production and loss under the steady-state assumption allows us to calculate the total N_2 1P VER. This balance can be described by the equation:

$$n_e n_{N_2}\left(k_{e,N_2(B^3\Pi_g)} + k_{e,N_2\left(B'^3\Sigma_u^-\right)} + k_{e,N_2(W^3\Delta_u)} + 0.5k_{e,N_2(C^3\Pi_u)}\right) = n_{N_2(B^3\Pi_g)}k_{N_2\,1P} \quad (1)$$

where n_X refers to the density of species or state X in cm^{-3}, $k_{e,Y}$ is the electron impact excitation of excited state Y from the ground state in cm^3/s (obtained from BOLSIG+), and $k_{N_2\,1P}$ is the radiative transition frequency for the N_2 1P transition in units of $1/\mathrm{s}$ (see Table S2). The term on the right hand side represents the N_2 1P volume emission rate in units of photons/cm^3/s.

GL emissions occur via relaxation of the $O(^1S)$ state to the $O(^1D)$ state. The $O(^1S)$ state can be excited by electron impact and by O quenching of $N_2\left(A^3\Sigma_u^+\right)$. $N_2\left(A^3\Sigma_u^+\right)$ is formed through electron impact excitation and radiative cascade from the $N_2\left(B^3\Pi_g\right)$ state. The $N_2\left(A^3\Sigma_u^+\right)$ state undergoes radiative decay to the N_2 ground state and is additionally quenched through collisions with O and O_2 (Campbell et al., 2006). This process is described by the equation:

$$n_e n_{N_2} k_{e,N_2\left(A^3\Sigma_u^+\right)} + n_{N_2(B^3\Pi_g)} k_{N_2\ 1P} = n_{N_2\left(A^3\Sigma_u^+\right)} \left(k_{VK} + n_O \left(k_{Q1} + k_{Q2} + k_{Q3}\right) + n_{NO} k_{Q4} + n_{O_2} k_{Q5}\right) \tag{2}$$

where k_{Qx} represents the rate coefficient for quenching reaction x in cm^3/s. These quenching reactions and their rates are listed in Table S1. k_{VK} is the radiative transition rate for the Vegard-Kaplan bands, given in Table S2. From the above equation, we can calculate the $N_2\,(A^3\Sigma_u^+)$ state density and determine the contribution to the $O(^1S)$ state from the quenching reaction.

Quenching of the $O(^1S)$ state is mainly caused by collisions with O_2, while quenching from other species has a minimal effect (less than 10%) at picket fence altitudes. However, we also include quenching by O and NO. The balance for $O(^1S)$ is expressed as:

$$n_e n_O k_{e,O(^1S)} + n_{N_2\left(A^3\Sigma_u^+\right)} n_O k_{Q1} = n_{O(^1S)} \left(k_{557.7\ \mathrm{nm}} + n_O k_{Q6} + n_{O_2} \left(k_{Q7} + k_{Q8}\right) + n_{NO} \left(k_{Q9} + k_{Q10}\right)\right) \tag{3}$$

where, again, the quenching reaction rates are given in Table S1 and the radiative transition rate $k_{557.7\ \mathrm{nm}}$ is given in Table S1. The total GL VER is obtained by solving the above equation for $n_{O(^1S)} k_{557.7\ \mathrm{nm}}$.

N_2^+ 1N emissions occur through electron impact ionization of N_2, followed by rapid relaxation of the resulting N_2^+ ion in the excited $N_2^+\,(B^2\Sigma_u^+)$ state to the ground state. Quenching is negligible at picket fence altitudes. Therefore, the electron impact excitation is the sole contributor to the N_2^+ 1N VER. We obtained electron impact excitation collisional cross sections for the $N_2^+\,(B^2\Sigma_u^+)$ state from Shemansky and Liu (2005).

Text S2. Calculating VERs for Various UV Emissions

We can extend our model to predict ultraviolet (UV) picket fence spectral features which may make good targets for future space-based observations. To do so, we calculate

VERs for the N_2 Vegard-Kaplan (VK), Lyman-Birge-Hopfield (LBH), and Second Positive (2P) bands, as well as the 1356 $\mathring{A}$ atomic oxygen emission (Meier, 1991; Liu & Pasko, 2005; Eastes, 2000). The dominant source of each of these emissions is direct electronic excitation which is calculated from BOLSIG+, as described in Section 3.2, as well as some cascade contributions from higher energy states, described below. We do not estimate the 1304 $\mathring{A}$ atomic oxygen emission due to complications arising from multiple scattering, which is beyond the scope of this study. Emissions from N and NO are not considered in this analysis.

The N_2 VK bands are generated by the relaxation of the $N_2\,(A^3\Sigma_u^+)$ state to the ground state, and the VK VER is obtained as part of our GL VER calculation (Equation 2). The N_2 2P emissions result from the relaxation of the $N_2\,(C^3\Pi_u)$ state to the $N_2\,(B^3\Pi_g)$ state, which we determined while examining the radiative cascade contribution to the N_2 1P VER (Equation 1).

The N_2 LBH bands (120-280 nm) form when the excited $N_2\,(a^1\Pi_g)$ state relaxes to the ground state. Since the quenching altitude for $N_2\,(a^1\Pi_g)$ is around 77 km, it is not significantly quenched at picket fence altitudes (Liu & Pasko, 2005). We do not consider the radiative and collisional cascades from $N_2\,(a'\,^1\Sigma_u)$ and $N_2\,(w^1\Delta_u)$, which could increase the LBH band system emissions by a factor of approximately 1.6 (Eastes, 2000).

The 1356 Å atomic oxygen emission occurs when the $O(3s^5S)$ state relaxes to its ground state. We also consider the cascade contribution from the higher $O(3p^5P)$ state, but disregard cascade from other higher quintet states. We also neglect the effects of multiple scattering and absorption from O_2, both of which can significantly reduce the total observable emissions depending on the observation geometry (Meier, 1991).

The full results of this modeling are shown in Figure S2. At 110 km and 55 Td, we find the N_2 VK, N_2 LBH, N_2 2P, and O 1356 Å to GL ratios to be 0.28, 0.24, 0.15, and 0.006, respectively. For the brightest event that we observed, which is about 7 kR in the GL after accounting for atmospheric transmission, we expect that only N_2 VK and LBH bands would emit enough to be observed while N_2 2P and O 1356 Å are likely not good targets for future observations. Any observational comparisons will additionally need to account for viewing angle, absorption, multiple scattering, and instrumental effects.

Figure S1

Figure S2

Table S1

Table S2

References

Campbell, L., Cartwright, D. C., Brunger, M. J., & Teubner, P. J. O. (2006). Role of electronic excited n2 in vibrational excitation of the n2 ground state at high latitudes. *J. Geophys. Res.: Space Phys.*, *111*(A9).

Eastes, R. W. (2000). Modeling the n2 lyman-birge-hopfield bands in the dayglow: Including radiative and collisional cascading between the singlet states. *J. Geophys. Res.: Space Phys.*, *105*(A8), 18557–18573.

Eyler, E., & Pipkin, F. (1983). Lifetime measurements of the $B^3\Pi_g$ state of N_2 using laser excitation. *J. Chem. Phys.*, *79*(8), 3654–3659.

Grubbs, G., Michell, R., Samara, M., Hampton, D., Hecht, J., Solomon, S., & Jahn, J.-M. (2018). A comparative study of spectral auroral intensity predictions from multiple electron transport models. *J. Geophys. Res.: Space Phys.*, *123*(1), 993–1005.

Liu, N., & Pasko, V. P. (2005). Molecular nitrogen LBH band system far-UV emissions of sprite streamers. *Geophysical Research Letters*, *32*(5).

Meier, R. (1991). Ultraviolet spectroscopy and remote sensing of the upper atmosphere. *Space Sci. Rev.*, *58*(1), 1–185.

Porter, H. S., Jackman, C. H., & Green, A. E. S. (1976). Efficiencies for production of atomic nitrogen and oxygen by relativistic proton impact in air. *Journal of Chemical Physics*, *65*, 154-167.

Shemansky, D. E., & Liu, X. (2005). Evaluation of electron impact excitation of $N_2 X^1\Sigma_g^+(0)$ into the N_2^+ $X^2\Sigma_g^+(v)$, $A^2\Pi_u(v)$, and $B^2\Sigma_u^+(v)$ states. *J. Geophys. Res.: Space Phys.*, *110*(A7).

Strickland, D., Bishop, J., Evans, J., Majeed, T., Shen, P., Cox, R., ... Huffman, R. (1999). Atmospheric ultraviolet radiance integrated code (auric): Theory, software architecture, inputs, and selected results. *Journal of Quantitative Spectroscopy and Radiative Transfer*, *62*(6), 689–742.

Vallance Jones, A. (1974). *Aurora*. D. Reidel publishing company.

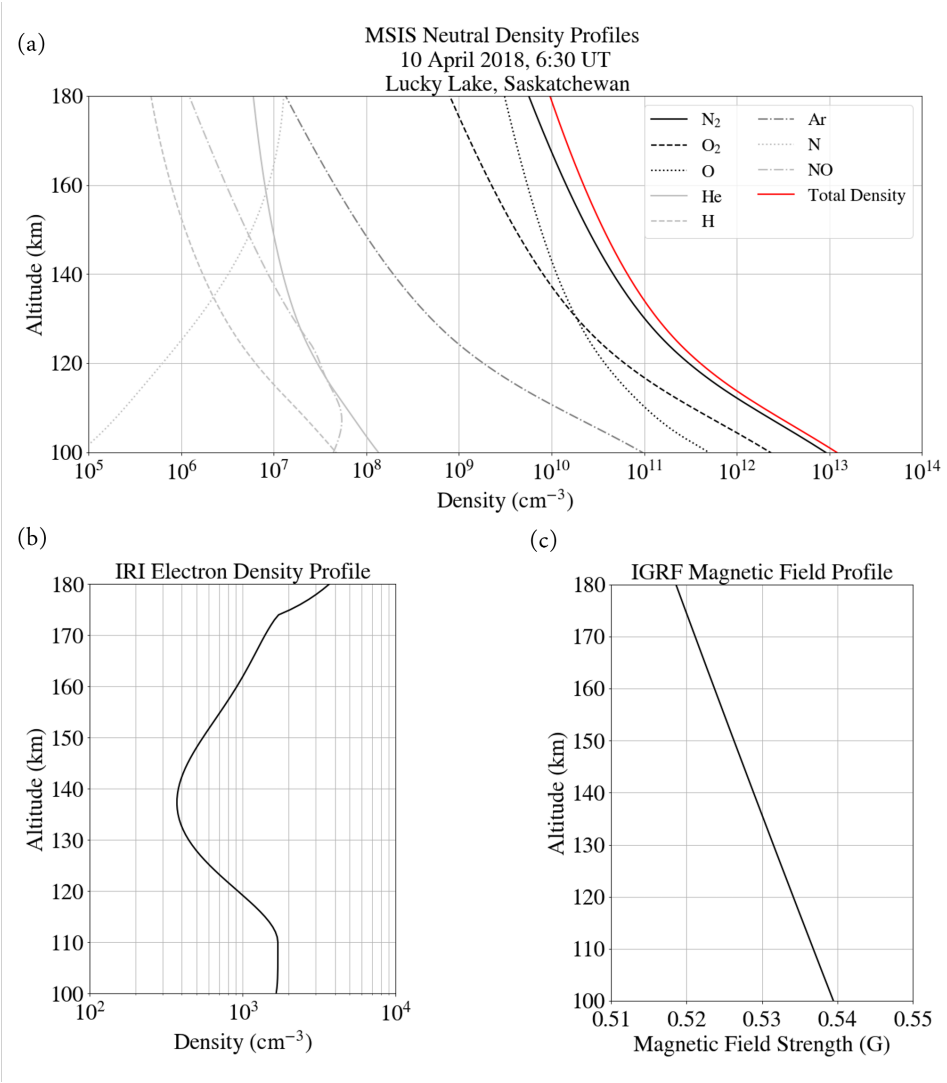

Figure S1. Modeled atmospheric and ionospheric profiles from the time and location of the TREx observations. (a) Neutral atmospheric density profiles from MSIS. (b) Electron density profile from IRI. (c) Magnetic field strength profile obtained from IGRF.

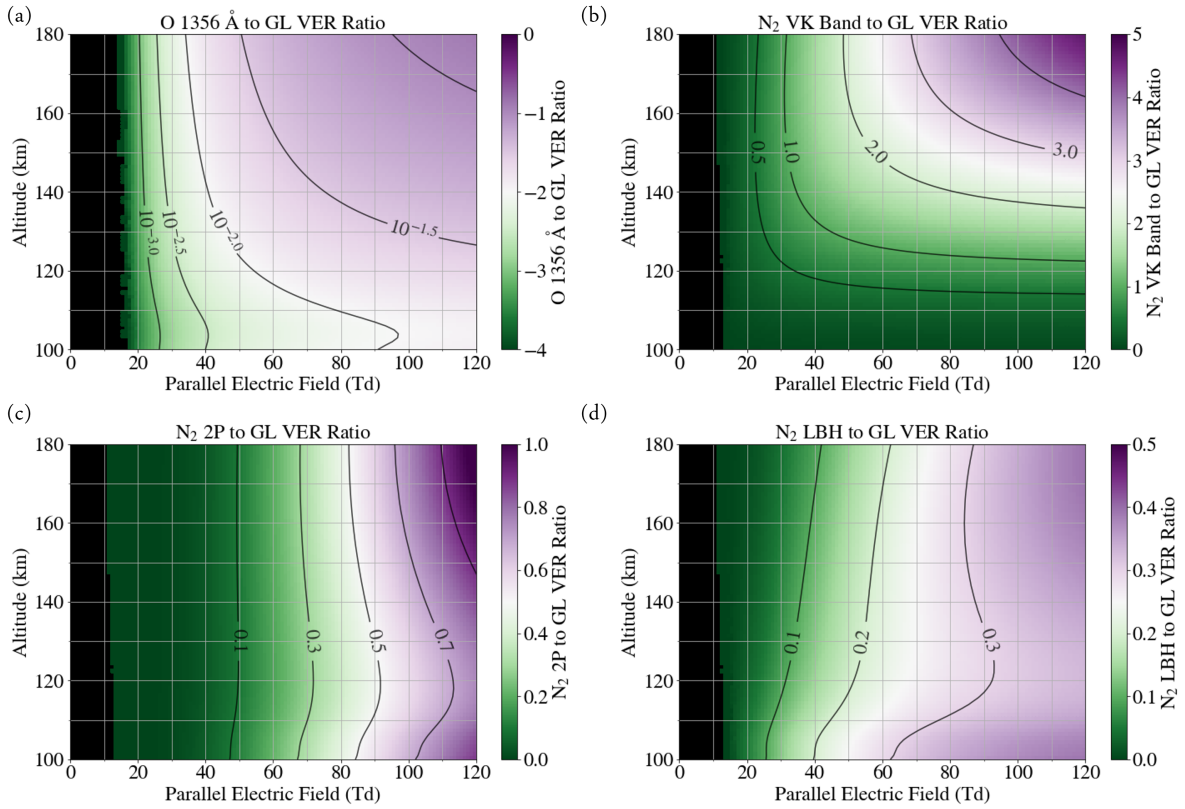

Figure S2. Calculated VER Ratios of various UV emissions to GL as a function of altitude and parallel electric field strength. (a) O 1356 Å (b) VK Bands (c) N_2 2P (d) N_2 LBH.

Reaction #	Quenching Reaction	Reaction Rate Constant (cm^3/s)	Source
Q1	$N_2\,(A^3\Sigma_u^+) + O \rightarrow N_2 + O(^1S)$	1×10^{-11}	Grubbs et al. (2018)
Q2	$N_2\,(A^3\Sigma_u^+) + O \rightarrow N_2 + O$	1.8×10^{-11}	Grubbs et al. (2018)
Q3	$N_2\,(A^3\Sigma_u^+) + O \rightarrow NO + N$	2×10^{-11}	Campbell et al. (2006)
Q4	$N_2\,(A^3\Sigma_u^+) + NO \rightarrow N_2 + NO$	8.9×10^{-11}	Grubbs et al. (2018); Strickland et al. (1999)
Q5	$N_2\,(A^3\Sigma_u^+) + O_2 \rightarrow N_2 + O_2$	4×10^{-12}	Grubbs et al. (2018); Strickland et al. (1999)
Q6	$O(^1S) + O \rightarrow O + O$	2×10^{-14}	Grubbs et al. (2018)
Q7	$O(^1S) + O_2 \rightarrow O + O_2$	$1.6 \times 10^{-12}\chi$[a]	Grubbs et al. (2018)
Q8	$O(^1S) + O_2 \rightarrow O(^1D) + O_2$	$7.2 \times 10^{-13}\chi$[a]	Grubbs et al. (2018)
Q9	$O(^1S) + NO \rightarrow O(^1D) + NO$	5.12×10^{-11}	Grubbs et al. (2018)
Q10	$O(^1S) + NO \rightarrow O(^1D) + NO$	2.88×10^{-11}	Grubbs et al. (2018)

Table S1. Quenching Reaction Rate Constants

[a] $\chi = e^{-\left(6750 - 0.0151T_n^2\right)/8.314T_n}$ where T_n is the neutral temperature in K.

Radiative Transition Reaction	Spectral Feature	Transition Rate (1/s)	Source
$N_2\,(B^3\Pi_g) \rightarrow N_2\,(A^3\Sigma_u^+) + h\nu_{N_2\,1P}$	N_2 First Positive Bands	2×10^5	Eyler and Pipkin (1983)
$N_2\,(A^3\Sigma_u^+) \rightarrow N_2\left(X^1\Pi_g^+\right) + h\nu_{VK}$	Vegard-Kaplan Bands	0.352	Grubbs et al. (2018)
$O(^1S) \rightarrow O(^1D) + h\nu_{557.7\,\mathrm{nm}}$	O Green Line (557.7 nm)	1.26	Grubbs et al. (2018)

Table S2. Radiative Transition Rates